

SILICATE EMISSION IN THE TW HYDRAE ASSOCIATION

MICHAEL L. SITKO¹

Department of Physics, University of Cincinnati, Cincinnati, OH 45221-0011; sitko@physics.uc.edu

AND

DAVID K. LYNCH¹ AND RAY W. RUSSELL¹

The Aerospace Corporation, Los Angeles, CA 90009-2957

Received 2000 July 6; accepted 2000 July 31

ABSTRACT

The TW Hydrae association is the nearest young stellar association. Among its members are HD 98800, HR 4796A, and TW Hydrae itself, the nearest known classical T Tauri star. We have observed these three stars spectroscopically between 3 and 13 μm . In TW Hya, the spectrum shows a silicate emission feature that is similar to many other young stars' with protostellar disks. The 11.2 μm feature indicative of significant amounts of crystalline olivine is not as strong as in some young stars and solar system comets. In HR 4796A, the thermal emission in the silicate feature is very weak, suggesting little in the way of (small silicate) grains near the star. The silicate band of HD 98800 (observed by us, but also reported by Sylvester & Skinner) is intermediate in strength between TW Hya and HR 4796A.

Key words: stars: individual (TW Hydrae, HR 4796A, HD 98800) — stars: pre-main-sequence — techniques: spectroscopic

1. INTRODUCTION

Since the discovery 15 years ago that a large fraction of all main-sequence stars possessed excess infrared emission (Aumann 1988), the study of these “Vega-type stars” and their precursors has grown enormously. With the detection of the edge-on debris disk in β Pictoris (Smith & Terrile 1984) and the equally important discovery that the debris exhibited a silicate emission band whose structure was similar to solar system comets (Knacke et al. 1993), it was apparent that at least some of these systems might be true planetary systems, perhaps similar to what our own solar system was like in its youth. Since that time, disks and tori around other stars have been successfully imaged.

Recently, Kastner et al. (1997) identified a previously unrecognized nearby young stellar association that consisted of five T Tauri (TT) or T Tauri-like stars, including the classical TT star TW Hydrae. Designated as the TW Hya association (TWA), the list of objects in this stellar group is now over a dozen objects and growing (Webb et al. 1999). Located at a distance of about 50 pc, TWA represents the nearest region of recent (< 20 Myr) star formation. It is no longer embedded in a molecular cloud, yet one of its members, TW Hya itself, possesses both a circumstellar molecular cloud (CO, HCN, and CN have been detected; Kastner et al. 1997) and an infrared excess. HR 4796A, which is also believed to be a member of TWA (Webb et al. 1999), has a dusty torus that has been recently resolved (Jayawardhana et al. 1998; Koerner et al. 1998; Schneider et al. 1999). Another member of TWA is HD 98800, a multiple star system with dust concentrated around one unresolved pair (Gehrz et al. 1999; Koerner et al. 2000). Combining a variety of criteria, Weintraub et al. (2000) derive an age of 5–15 Myr for TWA.

Because TWA is the nearest group of pre-main-sequence (PMS) stars known, it is providing imaging possibilities that

are, in some ways, superior to that of the Taurus-Auriga complex and at an epoch of great importance to the study of planet formation. This association provides a laboratory for studying a number of stars of the same age but with different masses, multiplicities, etc. Although the luminosities of low-mass stars in TWA are substantially less than those of younger stars of the same mass (such as in Taurus-Auriga), the relative proximity of the TW Hya association and the implementation of sensitive IR array detectors on large telescopes opens up a realm of study of PMS disk evolution not possible before.

In this paper, we report observations of the 3–13 μm spectra of TW Hya, HR 4796A, and HD 98800. The mid-IR spectrum of HD 98800 has already been reported by Sylvester & Skinner (1996) using ground-based data and by Walker & Heinrichsen (2000) using ISOPHOT. Our data extend to shorter wavelengths than the Sylvester & Skinner data, while having a better signal-to-noise ratio than the ISOPHOT observations. Both are useful for realistically determining the photospheric contribution to the observed emission.

2. OBSERVATIONS

Spectra of the TWA targets were obtained with the Aerospace Corporation's Broadband Array Spectrograph System (BASS) configured to $f/35$ at the 3 m NASA Infrared Telescope Facility (IRTF). The BASS consists of a pair of cooled prisms that disperse the spectrum onto two 58-element blocked impurity band linear arrays that simultaneously span the 3–13.5 μm region. The spectral dispersion ranges from about 30 to 125 over each of the 3–6 and 6.5–13.5 μm regions. At the IRTF, the BASS entrance aperture subtends $3''.4$. The observations of TW Hya were obtained on 1998 March 21 (UT). HD 98800 was observed on 1998 February 8 (UT), and HR 4796A was observed on 1998 May 12 (UT).

Details of the observations are listed in Table 1, and the resultant spectra are shown in Figures 1 (TW Hya), 2 (HD 98800), and 3 (HR 4796A), where we have plotted the spectral flux (λF_λ in watts per square meter). All BASS spectral

¹ Visiting Astronomer, NASA Infrared Telescope Facility, operated by the University of Hawaii under contract with the National Aeronautics and Space Administration.

TABLE 1
OBSERVING PARAMETERS

Date (UT)	Star	Mean UT	Mean Air Mass	Number of Spectra	Int. Time (minutes)
1998 Feb 8	HD 98800	1135	1.46	4	32
	Arcturus	1205	1.45	3	4
1998 Mar 21	Sirius	0800	1.75	5	8
	TW Hya	0856	1.75	16	53
1998 May 12	Pollux	0751	2.78	5	7
	HR 4796A	0855	2.16	16	53
	Vega	1034	1.40	6	8

data points, such as those in the atmospheric CO_2 and H_2O bands, with errors exceeding the observed flux (i.e., signal-to-noise ratio less than unity) have been rejected. The spectrum of TW Hya was flux-calibrated using observations of α CMa (Sirius) at approximately the same air mass, obtained just prior to the TW Hya data. The spectrum of HD 98800 was calibrated using observations of α Boo (Arcturus) at the

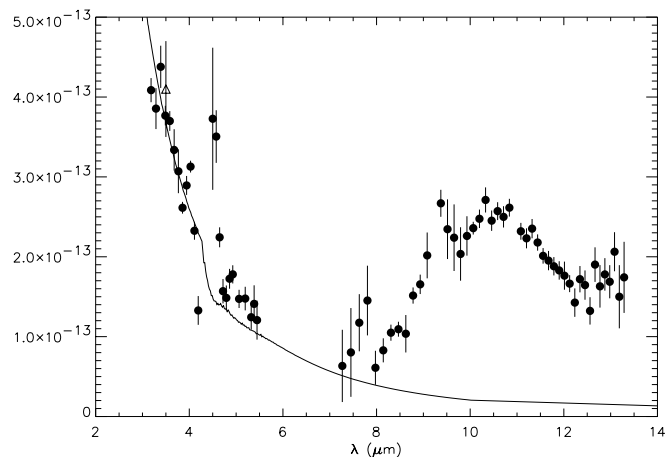


FIG. 1.—Spectrum of TW Hya (filled circles) from 3 to 14 μm , along with the L -band data of Rucinski & Krautter (1983, open triangle; barely visible among the BASS data) and the *IRAS* 12 μm data. No adjustments to the flux levels of any of the data have been made. For comparison, we also show the K7 model atmosphere ($T = 4000$ K, $\log g = 4.5$, $\log z = 0.0$). The model spectrum was generated using the 1991 Kurucz models, reproduced using the IUEDAC's KURUCZ91.PRO routine, and normalized to the L -band data of Rucinski & Krautter.

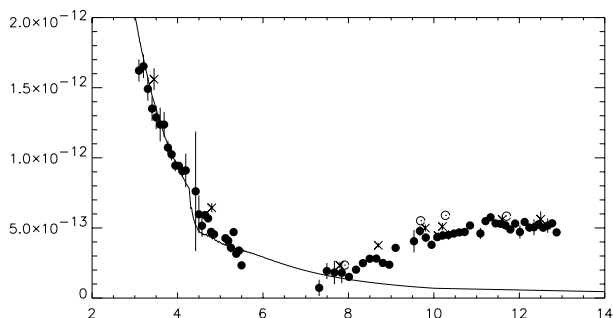


FIG. 2.—Spectrum of HD 98800 (filled circles) from 3 to 14 μm . Also shown is the appropriate model atmosphere ($T = 4250$ K, $\log g = 4.5$, $\log z = 0.0$), normalized to the flux at 3.5 μm . For comparison, we have also plotted the photometric data of Zuckerman & Becklin (1993) as crosses and Koerner et al. (2000) as open circles.

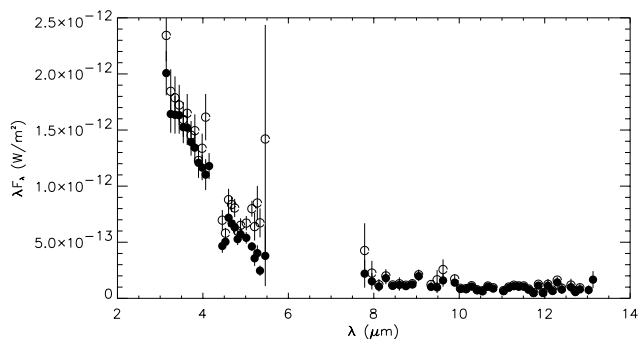


FIG. 3.—Spectrum of HR 4796A from 3 to 14 μm , calibrated using α Lyr (filled circles) and β Gem (open circles).

same air mass and converted to the same flux system using the Arcturus-to-Sirius flux ratio determined by Russell & Mazuk (1998) for the BASS instrument. For HR 4796A, no calibrator at the same air mass was observed. To establish the spectrum, it was calibrated against one star, α Lyr (Vega), at a lower air mass and another star, β Gem (Pollux), at a higher air mass. For the latter, we also used the Pollux-to-Sirius ratio of Russell & Mazuk (1998). Outside of those wavelengths, which are severely affected by telluric lines and are usually rejected from the figures because of their inferior signal-to-noise ratio (S/N), the resultant fluxes are nearly identical. We illustrate this fact by plotting both resultant spectra in Figure 3. Because of the similarity of these spectra, we have taken the mean values and plotted them against the appropriate model atmosphere spectrum in Figure 4. The detail near the 10 μm band is shown in Figure 5.

3. DISCUSSION OF THE SPECTRA OF INDIVIDUAL OBJECTS

3.1. TW Hydrae

Figure 6 shows the spectral energy distribution of TW Hya from 0.44 to 100 μm . The photometric data in the 12, 25, 60, and 100 μm bands were obtained by *IRAS*. In addition, measurements in the B , V , R , I , J , H , K , and L photometric bands by Rucinski & Krautter (1983) are included. Because TW Hya is a variable star, we show the mean value of the Rucinski & Krautter measurements, while the error bars indicate the range within those values. We also show the Kurucz model photosphere spectrum of a K7 V star, normalized to the K - and L -band flux.

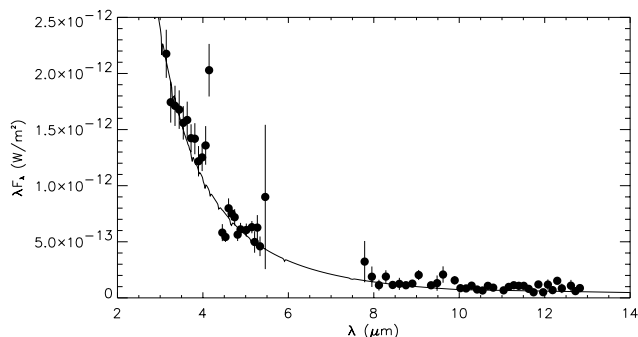


FIG. 4.—Spectrum of HR 4796A and the appropriate model atmosphere ($T = 9500$ K, $\log g = 4.0$, $\log z = 0.0$), normalized to the flux at 3.5 μm .

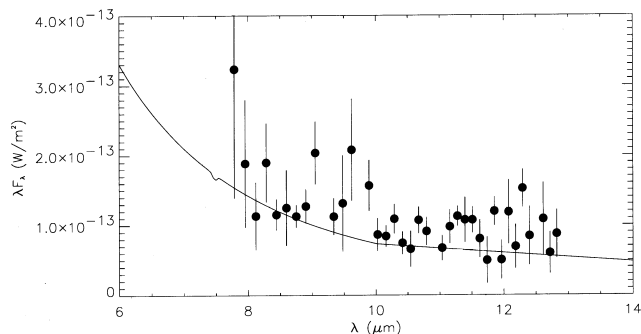


FIG. 5.—Spectrum of HR 4796A, detail near $10 \mu\text{m}$

As can be seen in Figure 6, TW Hya possesses a significant infrared excess. In fact, the emission longward of $8 \mu\text{m}$, which is dominated by the thermal emission of the circumstellar dust, accounts for 23% of the total observed luminosity of the star. Originally, Ruchinski & Krautter (1983) fitted the data at $1.25 \mu\text{m}$ and shortward with a blackbody spectrum, which left a flux excess between 1.25 and $3.5 \mu\text{m}$. However, model atmospheres of stars in this temperature range have line opacities that naturally reproduce the shape of the spectrum observed in this region. In Figure 6, we illustrate this by fitting a Kurucz model atmosphere of a K7 star and normalizing it to the $2\text{--}4 \mu\text{m}$ BASS data. The same model fit is included in Figure 1. The fit is not perfect down to the shortest wavelength, but TW Hya is a variable star, the BASS data are not simultaneous with the observations of Ruchinski & Krautter, and the star possesses a short-wavelength excess attributed to the disk-star boundary layer (Muzerolle et al. 2000), which we have not included here. In any case, there does not appear to be any significant excess flux between 2 and $8 \mu\text{m}$.

In TW Hya (see Fig. 1), the emission between 8 and $13 \mu\text{m}$ is dominated by the silicate band at $10 \mu\text{m}$. The three points between 9.5 and $9.8 \mu\text{m}$ with the large error bars lie in the telluric ozone band and may not be reliable, even though the data on TW Hya were obtained at the same air mass as that of Sirius. The point at $9.4 \mu\text{m}$ with the smaller error bar sits right at the edge of this band.

3.2. HD 98800

The spectrum of HD 98800 between 3 and $13.5 \mu\text{m}$ is shown in Figure 2. Also shown in the figure are the photometric data of Zuckerman & Becklin (1993) and Koerner et al. (2000). The agreement between absolute fluxes derived

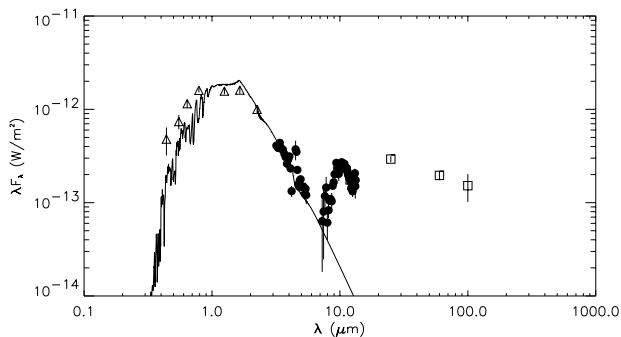


FIG. 6.—Total energy distribution of TW Hya from 0.44 to $100 \mu\text{m}$. The circles are data obtained with BASS. The triangles are the data of Ruchinski & Krautter (1983), and the squares are the *IRAS* photometry.

from the BASS data and the other two sets is good, although the BASS fluxes are slightly lower. The shape and total flux level is also the same as the spectral data obtained by Sylvester & Skinner (1996), whose observations cover the $8\text{--}24 \mu\text{m}$ region, and who used the photometry from another instrument in their modeling. The value of the BASS observations is that they cover the wavelength regions dominated by both photospheric and dust emission simultaneously and on the same photometric system, allowing the photospheric flux to be extrapolated out into the $10 \mu\text{m}$ region using a single set of simultaneous data. The ISOPHOT observations of Walker & Heinrichsen (2000) cover the $5.8\text{--}11.6 \mu\text{m}$ region but suffer from such large systematic fluctuations in the signal that the silicate feature cannot even be seen.

The BASS spectrum shortward of $6 \mu\text{m}$ is well fitted by the photospheric model normalized near $3 \mu\text{m}$. This is consistent with the results of Koerner et al. (2000), who fitted similar models to the individual A and B components of the system (each of which is a binary) and find that the flux is dominated by photospheric emission out to $7 \mu\text{m}$ in both A and B components.

3.3. HR 4796A

In Figures 4 and 5, we show the spectrum of HR 4796A and its appropriate model atmosphere. The $8\text{--}13.5 \mu\text{m}$ flux is weak, and half is photospheric. Koerner et al. (1998), using thermal imaging with the MERLIN instrument on Keck, derive a total flux at $12.5 \mu\text{m}$ of $5.4 \times 10^{-14} \text{ W m}^{-2}$, of which it was estimated that half was photospheric. For the BASS observations, the $12\text{--}13 \mu\text{m}$ flux is higher than those derived from MERLIN, but the fraction due to photospheric emission is comparable. The lack of any detectable excess flux shortward of $8 \mu\text{m}$ indicates that there is little dust hotter than 450 K or closer than about 2 AU (depending somewhat on the optical albedo and infrared emissivity of the grains). Augereau et al. (1999) have modeled the spectral energy distribution of HR 4796A, including the hot inner region, with a two-component dust model. In their model, the excess emission near $10 \mu\text{m}$ comes primarily from huge (larger than $100 \mu\text{m}$ in size) grains located near 9 AU from the star. Unfortunately, the quality of the spectra here is inadequate to discern the detailed spectral features expected from such material.

4. COMPARISON WITH SOLAR SYSTEM COMETS AND OTHER DUSTY PMS STARS

4.1. General Considerations

Some main-sequence and pre-main-sequence stars with dusty debris disks possess silicate grains whose spectral features resemble those of long-period comets. Knacke et al. (1993) were the first to demonstrate this by comparing the $10 \mu\text{m}$ emission feature in β Pic with 1P/Halley and Levy 1990 (C/1991 L3). All three objects exhibit an emission band with maxima or shoulders near 9.5 and $11.2 \mu\text{m}$, the latter indicative of crystalline olivine. Subsequently, Herbig Ae/Be stars (HAEBEs) embedded in star-forming regions have been examined (i.e., Hanner, Brooke, & Tokunaga 1995), and some, such as HD 150193 in the ρ Oph cloud, have been found to possess features of a similar nature. The two isolated HAEBEs (which might also be called post-HAEBEs since they are no longer embedded in nebulosity), HD 31648 and HD 163296, were shown to have spectra

similar to that of Hale-Bopp and Levy (Sitko et al. 1999). However, the stellar disk dust in these systems emitted more strongly near $9.4 \mu\text{m}$ than did the comets.

It should be remembered that in the case of a comet, we are dealing with material with a single well-defined distance from the Sun, while this is not the case for a disk. Nevertheless, Wooden et al. (2000) have shown that over a range of a factor of 3 in heliocentric distance, the spectral shape of Hale-Bopp was invariant, with the exception of one subfeature. Furthermore, a comparison of the *Infrared Space Observatory (ISO)* spectra of the HAEBE star HD 100546 and Hale-Bopp indicate that, while the overall spectral energy distributions are significantly different in the way expected (more cool dust in the stellar disk), the shapes of the narrow features are still quite similar (Malfait et al. 1998). However, the shape of the $10 \mu\text{m}$ band is sensitive to the abundance and form of pyroxenes, as evidenced in the variety of spectral shapes of pyroxene-rich interplanetary dust particles that have been analyzed in the laboratory (Sanford & Walker 1985; Bradley, Humecki, & Germani 1992). It is interesting that the one subfeature that was observed to vary with heliocentric distance in Hale-Bopp has been attributed to crystalline pyroxenes (Wooden et al. 2000). This suggests that perhaps the main reason for the excess $9.4 \mu\text{m}$ emission of the disks compared with comets is the presence of dust at temperatures much higher than those generally observed in solar system comets, which allows the crystalline pyroxenes to be enhanced but on a grander scale than was seen in Hale-Bopp.

4.2. TW Hydrae

In Figure 7, we show the $10 \mu\text{m}$ band of TW Hya, normalized to the continuum by dividing by a graybody that matches the observed flux at 8 and $13 \mu\text{m}$. Also shown are the data for HD 31648, HD 163296, comet Hale-Bopp, and comet Levy from Sitko et al. (1999). Although the data for TW Hya have a modest S/N, it is apparent that TW Hya does not have the same shape as the other objects. In particular, the well-defined crystalline olivine feature seen at $11.2 \mu\text{m}$ in both the comets and HD 31648 and HD 163296 seems to be considerably less defined in TW Hya. At best, a modest change of spectral slope is present at that wavelength. In Figure 8, we compare the spectrum of TW Hya with three HAEBEs (Sitko et al. 2000) whose emission features are representative of the wide variety that are seen in these PMS objects (excluding objects dominated by organic emission features). RY Tau exhibits a silicate feature that is

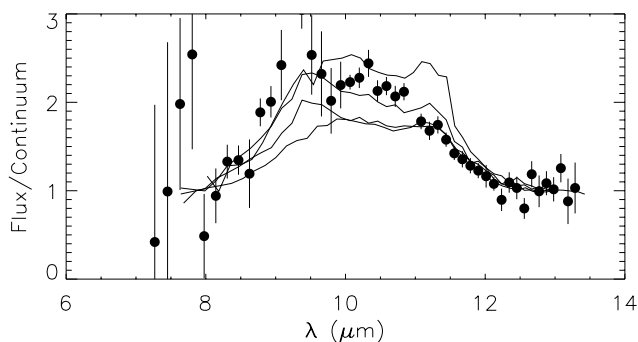


FIG. 7.—Flux-to-continuum ratio for TW Hya (circles) compared with those of HD 163296 (top thin line), HD 31648 (bottom thin line), comet Hale-Bopp (top thick line), and comet Levy (bottom thick line).

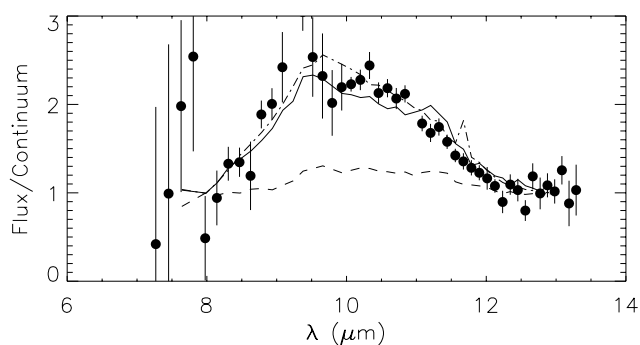


FIG. 8.—Flux-to-continuum ratio for TW Hya (circles) compared with that of HAEBEs with a wide variety of spectral shapes: HD 163296 (solid line), HD 35187 (dashed line), and RY Tau (dot-dashed line).

strong and relatively featureless, except for a single maximum near $9.7 \mu\text{m}$. In HD 163296 (again), the olivine feature is present but not as prominent as in comets, such as Hale-Bopp and Levy. Finally, the spectrum of HD 35187 has a weak silicate band but is more comet-like (flat-topped) in shape. In Figure 9, we also compare the spectrum of TW Hya with that of RW Aur, a PMS G5e star with circumstellar CO emission in the first vibrational overtone band (Sitko & Hanson 2000). Because the strength of the silicate band with respect to the underlying continuum in RW Aur is only one-quarter that of TW Hya, the band strength with respect to the continuum in RW Aur has been scaled up by a factor of 4 for comparison purposes.

Of the four “comparison” stars, the silicate band in TW Hya is most similar in shape and strength to that of RY Tau, an F8 Ve PMS star in the Taurus-Auriga cloud. The spectral shape in the silicate band of TW Hya is also nearly identical to that of RW Aur (G5e), but its strength is considerably stronger. This should not be construed to imply that TW Hya and the other late-type PMS stars are systematically different from the earlier type HAEBEs. Most HAEBEs are not strong $11.2 \mu\text{m}$ emitters. Furthermore, high-quality mid-IR spectra on a large sample of T Tauri stars are lacking.

In Figure 10, we show the flux-to-continuum ratio of HD 98800 with that of TW Hya. While the two sets of data overlap reasonably well between 11 and $13 \mu\text{m}$, much of this may simply be due to the normalization procedure used to obtain the flux-to-continuum ratio. Overall, the band strength seems to be weaker in HD 98800, and there may be

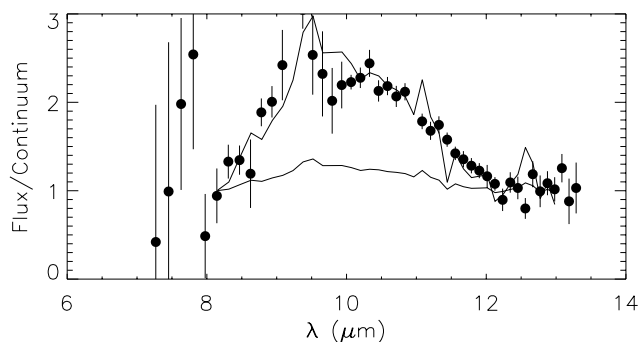


FIG. 9.—Flux-to-continuum ratio of TW Hya (circles) compared with that of RW Aur (solid line). The flux-to-continuum ratio of RW Aur has been scaled by a factor of 4 in this figure.

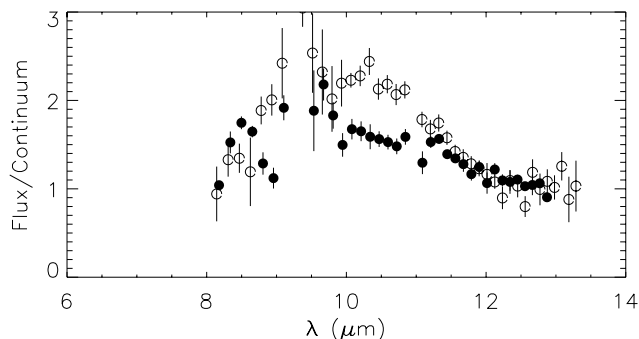


FIG. 10.—Flux-to-continuum ratio of HD 98800 (*filled circles*) compared with that of TW Hya (*open circles*).

structural differences as well. However, when the band strength is intrinsically weak, the normalization procedure tends to magnify the systematic effects in the data (such as small errors in cancellation of telluric lines between target and calibration star) so that spectral “features” may not be real. In such cases, a direct comparison of the observed fluxes may be more useful. In Figure 11, we compare the observed fluxes of these two stars directly (after suitable rescaling). Here the differences are more readily apparent.

Because of the weakness of the dust emission in HR 4796A compared with the extrapolated photospheric flux, the flux-to-continuum ratio was not determined.

5. DISCUSSION

In Figure 11, we compare the spectra of all three stars, normalized to the same flux between 3 and 5 μm , where all three are dominated by photospheric emission. It is apparent that the net strength of the silicate emission feature of the dust surrounding the three TWA stars is different, and it cannot simply be the result of differing ages, since the stars are believed to be approximately coeval. Thus, the degree to which small silicate grains survive and/or are modified in these systems must be dependent on other parameters as well, such as stellar mass, presence and location of companions, and the like. With only three TWA stars observed so far, it is premature to draw any specific conclusions in this regard. Furthermore, the quality of the spectra of the dust in HR 4796A and HD 98800 precludes any sweeping generalizations concerning their detailed mineralogies. Instead, we examine some of the inferences that can be made con-

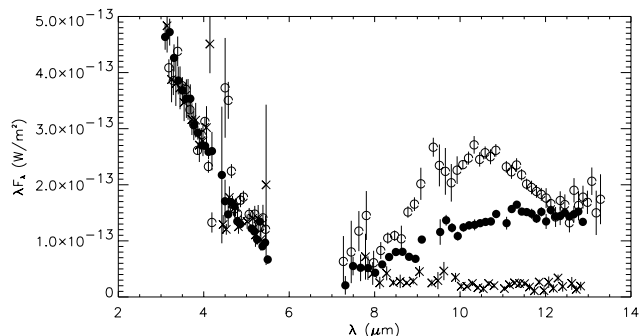


FIG. 11.—Observed flux of HD 98800 (*filled circles*), TW Hya (*open circles*), and HR 4796A (*crosses*) compared directly. In this figure, the flux of HD 98800 has been scaled down by a factor of 3.5, and that of HR 4796A by a factor of 4.5.

cerning the general nature of the material surrounding TW Hya specifically.

The 11.2 μm crystalline olivine feature has not been detected with the *ISO* Short Wavelength Spectrometer (SWS) in the emission spectra of the youngest (i.e., embedded) PMS stars but has been observed in a number of more evolved objects (Waelkens et al. 2000). Because the majority of the objects observable with the *ISO* SWS must be bright, most of the targets have been HAEBEs. The TTSs are too faint for SWS (van den Ancker 2000). Only a few have been observed at more modest spectral resolution with ISOPHOT (see Natta, Meyer, & Beckwith 2000), but many of these data have inadequate signal-to-noise ratios to make any conclusions regarding the presence of crystalline material.

The dust in TW Hya itself does not appear to exhibit the degree of crystallinity, as judged by the strength of the 11.2 μm olivine feature, that some other objects with resolved debris disks have and that is seen in many, *but not all*, solar system comets (Hanner, Lynch, & Russell 1994). For example, in the HAEBE star HD 163296, a star whose age is believed to be between 4 and 6 Myr, the feature is definitely present (Sitko et al. 1999; van den Ancker et al. 2000). About half (or more) of long-period comets studied so far also possess the 11.2 μm feature. These comets have their recent origin in the Oort cloud and were, presumably, originally formed in the Uranus-Neptune region of the early solar system. By contrast, short-period comets, whose origin is probably in the Kuiper belt, tend to have weaker silicate features (Lynch, Hanner, & Russell 1992; Lynch et al. 1995; Lynch, Russell, & Sitko 2000; Hanner et al. 1996). The mean particle sizes must be greater (or the feature otherwise hidden in some fashion) in these latter objects, and the degree of crystallinity cannot be assessed.

When does the crystalline material form in these disk systems, if at all? Bradley et al. (1999) have demonstrated that the most primitive unequilibrated interplanetary dust particles, of presumed cometary origin, exhibit a smooth silicate band essentially devoid of crystalline features. This is consistent with their glassy internal structure. The spectra of these particles resemble those of disk systems that do not exhibit the 11.2 μm feature. However, the large porous grains in which they are embedded, *along with significant amounts of crystalline material*, have spectra that resemble those older disk systems and solar system comets that do exhibit this crystalline feature. It may be that much of the crystalline material is produced early in the development of the protosolar nebula and is later agglomerated with the more pristine material (Bradley et al. 2000). One could even envision a scenario whereby disk or comet dust shed and heated near the star is recycled over the entire lifetime of the formation of the bulk of the cometesimals in the nebula. In such a scenario, “pristine” objects might be highly “contaminated” by dust processed at a variety of temperatures.

The lack of this feature in TW Hya, whose age is greater than that of some other stars exhibiting it, could be due to a number of factors. Perhaps it is simply too young, and has not entered the stage at which this material is produced. We simply do not have enough data on lower mass stars to know for sure whether they are slower than the higher mass stars in entering this phase (and not all of them do, to the best of our knowledge), or perhaps the material is currently not being delivered close enough to the star yet for the

material to emit strongly. In addition, the sheer *volume* of space surrounding the higher mass stars that is capable of thermally processing grains is larger than in lower mass stars.

6. CONCLUSION

We have presented 3–13 μm spectra of three stars in the TW Hya association: TW Hya, HR 4796A, and HD 98800. TW Hya possesses a strong silicate emission band that is generally similar in strength and shape to many other pre-main-sequence stars, such as HAEBEs and T Tauri stars. However, the feature does not show the unambiguous presence of crystalline material, as evidenced by the 11.2 μm feature, as is observed in some HAEBEs and in some long-period solar system comets. HR 4796A has only a very weak excess emission above photospheric levels, and nothing can be said about the presence of a significant silicate band from these data. HD 98800 is intermediate between these two in terms of the strength of its silicate band, but the data are inadequate to say anything about the mineralogy or degree of crystallinity.

For the object where we have the best data, TW Hya, the lack of obvious crystallinity is not entirely surprising, as it is absent in all of the youngest pre-main-sequence stars and in most, but not all, of the older ones. It is present in many of the long-period comets of our own solar system, however, and our failure to detect it so far in a younger star of

roughly solar mass is intriguing, though not unexpected. We are far from understanding how the crystalline material is produced and incorporated into the grains of our own solar system and in the disk systems of some of the higher mass stars.

One of the main obstacles preventing more definitive conclusions is the lack of high-quality mid-IR spectra of TTs. Many can be reached using ground-based instruments, but require long (in excess of an hour or two) integration times to achieve the necessary signal-to-noise ratio. A truly comprehensive study will require an instrument like the *Space Infrared Telescope Facility*.

Support for this work was provided for M. L. S. through NASA's Origins of Solar Systems Program grant NAG 5-9475 and the University Research Council and physics department of the University of Cincinnati. Support for D. K. L. and R. W. R. was provided by the Aerospace Corporation's Independent Research and Development program. We would like to thank Ann Mazuk and Ted Tessensohn for technical support and Bill Golisch and Dave Griep of the IRTF for expert telescope operation. The authors would also like to thank Robert Joseph for being flexible in the scheduling of the IRTF time for this project with our other programs. We also thank Carol Grady for her comments on the manuscript. The *IRAS* broadband fluxes were obtained via SIMBAD.

REFERENCES

- Augereau, J. C., Lagrange, A. M., Mouillet, D., Papaloizou, J. C. B., & Gorod, P. A. 1999, *A&A*, 348, 557
- Aumann, H. H. 1988, *AJ*, 96, 1415
- Bradley, J. P., Humecki, H. J., & Germani, M. S. 1992, *ApJ*, 394, 643
- Bradley, J. P., Keller, L. P., Flynn, G. J., & Sitko, M. L. 2000, in *ASP Conf. Ser. 196, Thermal Emission Spectroscopy and Analysis of Dust, Disks, and Regoliths*, ed. M. L. Sitko, A. L. Sprague, & D. K. Lynch (San Francisco: ASP), 119
- Bradley, J. P., et al. 1999, *Science*, 285, 1716
- Gehr, R. D., Smith, N., Low, F. J., Krautter, J., Nollenberg, J. G., & Jones, T. J. 1999, *ApJ*, 512, L55
- Hanner, M. S., Brooke, T. Y., & Tokunaga, A. T. 1995, *ApJ*, 438, 250
- Hanner, M. S., Lynch, D. K., & Russell, R. W. 1994, *ApJ*, 425, 274
- Hanner, M. S., Lynch, D. K., Russell, R. W., Hackwell, J. A., Kellogg, R., & Blaney, D. 1996, *Icarus*, 124, 344
- Jayawardhana, R., Fisher, S., Hartmann, L., Telesco, C., Piña, R., & Fazio, G. 1998, *ApJ*, 503, L79
- Kastner, J. H., Zuckerman, B., Weintraub, D. A., & Forville, T. 1997, *Science*, 277, 67
- Knacke, R. F., Fajardo-Acosta, S. B., Telesco, C. M., Hackwell, J. A., Lynch, D. K., & Russell, R. W. 1993, *ApJ*, 418, 440
- Koerner, D. W., Jensen, E. L. N., Cruz, K. L., Guild, T. B., & Gulktekin, K. 2000, *ApJ*, 533, L37
- Koerner, D. W., Ressler, M. E., Werner, M. W., & Backman D. E. 1998, *ApJ*, 503, L83
- Lynch, D. K., Hackwell, J. A., Edelsohn, D., Lahuis, F., Roelfsema, P. R., Wesselius, P. R., Walker, R. G., & Sykes, M. V. 1995, *Icarus*, 114, 197
- Lynch, D. K., Hanner, M. S., & Russell, R. W. 1992, *Icarus*, 97, 269
- Lynch, D. K., Russell, R. W., & Sitko, M. L. 2000, *Icarus*, 144, 187
- Malfait, K., Waelkens, C., Waters, L. B. F. F. M., Vandenbussche, B., Huygen, E., & de Graauw, M. S. 1998, *A&A*, 332, L25
- Muzerolle, J., Calvet, N., Briceño, C., Hartmann, L., & Hillenbrand, L. 2000, *ApJ*, 535, L47
- Natta, A., Meyer, M. R., & Beckwith, S. V. W. 2000, *ApJ*, 534, 838
- Rucinski, S. M., & Krautter, J. 1983, *A&A*, 121, 217
- Russell, R. W., & Mazuk, A. L. 1998, in *Proc. 8th Symp., Infrared Radiometric Sensor Calibration* (Logan: Space Dynamics Lab, Utah State Univ.)
- Sanford, S. A., & Walker, R. M. 1985, *ApJ*, 291, 838
- Schneider, G., et al. 1999, *ApJ*, 513, L127
- Sitko, M. L., Grady, C. A., Lynch, D. K., Russell, R. W., & Hanner, M. S. 1999, *ApJ*, 510, 408
- Sitko, M. L., & Hanson, M. M. 2000, in preparation
- Sitko, M. L., Lynch, D. K., Russell, R. W., Grady, C. A., & Hanner, M. S. 2000, in preparation
- Smith, B. A., & Terrile, R. J. 1984, *Science*, 226, 1421
- Sylvester, R. J., & Skinner, C. J. 1996, *MNRAS*, 283, 457
- van den Ancker, M. E. 2000, in *ASP Conf. Ser., Disks, Planetesimals and Planets*, ed. F. Garzón, C. Eiroa, D. de Winter, & T. J. Mahoney (San Francisco: ASP), in press
- van den Ancker, M. E., Bouwman, J., Wesselius, P. R., Waters, L. B. F. M., Dougherty, S. M., & van Dischoeck, E. F. 2000, *A&A*, 357, 325
- Waelkens, C., Malfait, K., Waters, L. B. F. M., & Meeus, G. 2000, in *ASP Conf. Ser. 196, Thermal Emission Spectroscopy and Analysis of Dust, Disks, and Regoliths*, ed. M. L. Sitko, A. L. Sprague, & D. K. Lynch (San Francisco: ASP), 53
- Walker, H. K., & Heinrichsen, I. 2000, *Icarus*, 143, 147
- Webb, R. A., Zuckerman, B., Patience, J., White, R. J., Schwartz, M. J., McCarthy, C., & Platais, I. 1999, *ApJ*, 512, L63
- Weintraub, D. A., Saumon, D., Kastner, J. H., & Forveille, T. 2000, *ApJ*, 530, 867
- Wooden, D. H., Butner, H. M., Harker, D. E., & Woodward, C. E. 2000, *Icarus*, 143, 126
- Zuckerman, B., & Becklin, E. E. 1993, *ApJ*, 406, L25